

## Heat Transfer Coefficient and Pressure Characteristics in a Copper Pipe Flow System: A Preliminary study Utilizing an EG/Water Mixture

Akhmad Junaedi<sup>1</sup>, Arif Rahman<sup>1</sup>, Sukarman<sup>1,2\*</sup>, Khoirudin<sup>1,2</sup>, Muhamad Taufik Ulhakim<sup>1,2</sup>, Renata Lintang Azizah<sup>3</sup>

<sup>1</sup>Department of Mechanical Engineering, Faculty of Engineering, Universitas Buana Perjuangan Karawang, Jl. HS.Ronggo Waluyo, Puseurjaya, Telukjambe Timur, Karawang, 41361 West Java, Indonesia.

<sup>2</sup>Centre of Research and Innovation in Energy Conversion and Nano Technology, Universitas Buana Perjuangan Karawang, 41361, West Java, Indonesia.

<sup>3</sup>Department of Mechanical Engineering Education, Faculty of Technology and Vocational Education Universitas Pendidikan Indonesia, 41361, West Java, Indonesia.

### ABSTRACT

This study investigates the performance of an ethylene glycol/water (EG/Water) fluid at a 40:60 volume ratio, a commonly used base fluid in heating and cooling systems. The evaluation focuses on analyzing heat transfer coefficients and pressure drops. The research adopts an experimental approach, utilizing a test section made of pure copper with an inner diameter of 16 mm, an outer diameter of 19 mm, and a length of 1500 mm. The volume ratio of EG/Water at 40:60 is an input parameter, along with varying fluid flow rates controlled by a valve, ranging from 2 to 18 liters per minute (LPM). Two tubular heaters with a combined capacity of 2000 W are attached to the copper pipe, regulated by a 3000 W voltage regulator. Electric current is measured with amperemeter. The temperature inlet of EG/Water was set in 60°C. The experimental results reveal that the heat transfer coefficient of the EG/Water fluid increases as the fluid flow rate rises. The highest heat transfer coefficient is achieved at 18 LPM, while the lowest is observed at 4 LPM. Pressure drops increases with higher flow rates, but this does not significantly affect the friction factor, as it undergoes a noticeable decrease while the Reynolds number increases.

**Keywords:** Friction factor, Reynolds number, Ethaline Glycol/Water, heat transfer coefficient, Pressure drops

### Article information:

- Submitted: 22/10/2023
- Revised: 22/12/2023
- Accepted: 24/12/2023

### Author correspondence:

\* ✉:

[sukarman@ubpkarawang.ac.id](mailto:sukarman@ubpkarawang.ac.id)

### Type of article:

- Research papers  
 Review papers

This is an open access article under the [CC BY-NC](https://creativecommons.org/licenses/by-nc/4.0/) license



## 1. INTRODUCTIONS

Heat transfer plays a pivotal role in numerous thermal applications, particularly in heating and cooling systems, where comprehending the process of heat transfer between copper pipes and the flowing fluids is of paramount importance [1]. The efficiency of heat transfer has a substantial impact on the overall performance of a system. The common practice of using a blend of ethylene glycol (EG) and Water (Water) in various cooling systems is aimed at fine-tuning the fluid's thermal properties and viscosity, factors that significantly influence the heat transfer process [2]. Consequently, exploring the optimal mixture ratios becomes essential in advancing the development of systems that are not only more efficient but also more effective. The heat transfer coefficient is a crucial metric for assessing a fluid's capacity to transfer heat. It is, therefore, imperative to elucidate how the EG/Water ratio in this mixture impacts the heat transfer coefficient. Furthermore, the use of the EG/Water blend can also alter the viscosity and flow characteristics of the fluid, subsequently affecting the pressure required to propel the fluid through the piping system [3]. Hence, gaining an understanding of the implications of these mixtures on pressure drop within the pipe becomes a matter of great significance.

The heat transfer coefficient is an essential factor that measures the rate at which heat is transferred across a surface and the medium of fluid [4, 5]. It denotes the capacity of the fluid to conduct heat and is an important factor for assessing the effectiveness of heat transfer processes [6, 7]. The heat transfer coefficient is influenced by a variety of factors, including fluid attributes, conditions of flow, and surface characteristics [8, 9]. It is affected by parameters such as fluid velocity [10-12], density [13], viscosity [14], thermal conductivity [15], and the presence of nanoparticles throughout the fluid [16, 17]. An accurate understanding of the heat transfer coefficient is essential when designing and optimizing cooling systems [18], heat exchangers [17], and other heat transfer devices, as it has an immediate effect on the overall heat transfer rate [19] and efficiency [20].

Heat exchangers find widespread application in a variety of industrial and residential settings, including power plant boilers as well as vehicle and building air conditioning systems [21]. To ensure the efficient operation of these systems, engineers require accurate correlations to optimize the design of these heat exchangers. Achieving maximum efficiency entails striking a delicate balance between high heat transfer rates and minimal pressure drops [22]. During the design phase, engineers have the option to choose between two flow regimes: laminar flow, which yields lower heat transfer rates and pressure drops, or turbulent flow, offering higher heat transfer rates and pressure drops [23]. Despite the usual practice of separately analyzing pressure drop and heat transfer, it's essential to recognize that there exists a direct and frequently underestimated relationship between these two factors [20].

Ethylene glycol and Water based fluids are solutions of ethylene glycol/water ((EG/Water) [24]. These fluids are frequently used heat transfer agents in various applications, including HVAC systems, automotive engines, and industrial processes. The ethylene glycol can influence the performance of EG/Water-based fluids to water ratio, also known as the ratios of EG in the mixture. The ratio selected may differ depending on implementation's specific needs, including for freeze protection or the desired operational temperature range.

Numerous studies have explored the performance of EG/Water mixtures. For instance, Manik et al. [25], investigated a 40:60 volume ratio of EG/Water for serving as the cold fluid and Water as the hot fluid in a heating/cooling system. The investigation explored using a radiator with various discharge rates for the hot fluid, ranging from 6.7 LPM to 27 LPM. In a different investigation, Abolarin et al. researched the heat transfer and pressure drop performance when using alternating twisted tape inserts in section tests with various flow regimes (Figure 1) [26]. The experiments utilized Water as fluid and were controlled under constant heat flux parameters, ranging from 1.35 kW/m<sup>2</sup> to 4 kW/m<sup>2</sup>, covering Reynolds numbers from 300 to 11,404. This extensive range encompassed turbulent flow, laminar, and transitional regimes [26].

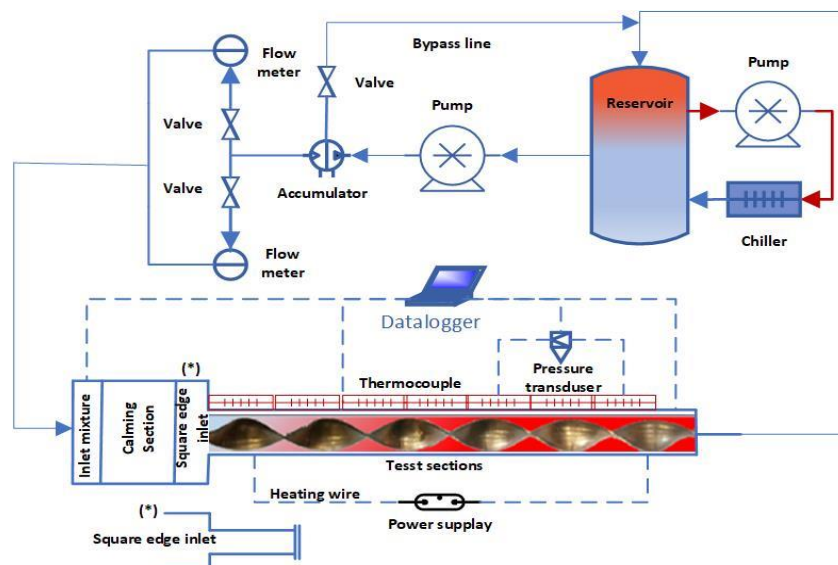


Figure 1. A visual representation of the experimental configuration adapted from [26].

Furthermore, various researchers in the field have carried out by Ghozatloo et al. [9], explored nanofluids with EG/Grn ratios, encompassing varying volume concentrations from 0.1% to 1.5%. They tested heat transfer coefficients using a shell and tube heat exchanger (STHE), where EG/Grn and EG were used as cold and hot fluids. The data derived from their analysis were compared with EG-based nanofluids. Azari et al. [27] conducted a study that specifically focused on heat transfer coefficients and overall heat transfer coefficients utilizing a 40:60 EG/Water ratio. They adopted an experimental approach and utilized a test section with a compact heat exchanger. Their experimental data analysis results were compared with a Water-based fluid's performance.

This study focuses on a preliminary investigation to optimize the utilization of a basic fluid mixture comprising ethylene glycol and water to determine the heat transfer coefficient while simultaneously lowering the mixture's freezing point. This research endeavor holds the potential to contribute significantly to the ongoing exploration of EG/water-blended fluids. It is worth noting that the existing literature lacks an in-depth analysis of heat transfer coefficients and friction factors in single-pipe systems employing EG/water mixtures. In this context, our research evaluates heat transfer coefficients (HTC) and friction factors for a 40:60 EG/water volume ratio with an operational temperature of 60°C. This experimental research, encompassing various fluid flow rate variations, is poised to offer novel insights into enhancing the efficiency of heat transfer systems that rely on EG/water-based fluid mixtures. Incorporating additives such as nanoparticles to enhance heat transfer characteristics holds significant promise for boosting heat transfer efficiency, particularly when transitioning from systems with relatively low heat transfer rates to higher-efficiency setups.

## 2. METHOD

### 2.1. Properties of Ethylene Glycol and Water

The thermal and physical characteristics of EG/ water mixture play a crucial role in a wide range of industrial and scientific applications, particularly in heat transfer and fluid dynamics [28]. Ethylene glycol has a melting point of -13°C, a boiling point of 197.3°C. At 20°C, ethylene glycol is distinguished as an exceptional heat transfer fluid due to its density of 1113.4 kg/m<sup>3</sup>, a significant specific heat capacity of about 2430 J/kg.K, and a notable thermal conductivity of 0.25 (W/m.K). In contrast, water at the same temperature excels as a heat storage medium owing to its high specific heat capacity of roughly 4180 J/kg.K and relatively elevated density of 998.2 kg/m<sup>3</sup>, allowing it to retain substantial thermal energy, combined with a commendable thermal conductivity of 0.606 W/m.K [29]. A thorough understanding of these properties is essential when designing systems that use EG and Water as coolants, heat transfer fluids, or for various industrial applications. Table 1 presents the thermophysical properties data for Ethylene glycol.

Table 1. The thermophysical properties of ethylene glycol/Water mixture with a volume ratio of 40:60 [31].

Temperature (K)	Density (kg/m <sup>3</sup> )	Viscosity (Pa.s)	Heat Specific (J/kg. K)	Thermal conductivity (W/m. K)
303	1041.3	0.00219	3674	0.441
308	1039.1	0.00188	3688	0.445
313	1036.8	0.00163	3702	0.450
318	1034.4	0.00143	3716	0.453
323	1031.8	0.00126	3730	0.457
328	1029.2	0.00113	3745	0.460
333	1026.4	0.00101	3759	0.463
338	1023.5	0.00092	3773	0.466
343	1020.4	0.00083	3787	0.469

## 2.2. Experimental Set up

The test section is constructed of pure copper pipe with a thickness and inner diameter of 1.5 mm and 18 mm, respectively.  $T_1$ - $T_{10}$  K-type thermocouples are strategically placed along the copper test section. Two thermocouples placed at the inlet ( $T_i$ ) and outlet ( $T_o$ ). Pressure sensors are installed to measure the difference in pressure between the inlet ( $P_i$ ) and outlet ( $P_o$ ). A centrifugal pump is integrated to facilitate the EG/Water mixture flow through the copper test section. The data logger recorded pressure, and temperature data with an accuracy of 0.1 psi, and  $0.25^\circ\text{C}$  respectively. The heater is controlled by a Voltage Regulator with input voltage specs of 220VAC, 50/60Hz, and an output voltage range of 0-250VAC. The copper pipes are heated by two tubular heater units, each with a 2000 W power capacity.

The calibration of all measurement instruments is the first step in the data collection process. A mixture of EG (ethylene glycol) and water in a 40:60 ratio is introduced into a 20-liter capacity tank and circulated through the experimental system until the pipes and hoses are filled. It circulated and was powered by a centrifugal pump. The data logging is set to record at 1-second intervals. At an inlet temperature of  $60^\circ\text{C}$ , the heaters are activated simultaneously, initiating the data recording process for temperature, pressure, and fluid flow rate. This system's chiller is a heat exchanger to maintain controlled inlet temperature conditions at  $60^\circ\text{C}$  and ensure it remains within specified parameters. Temperature, pressure, and flow rate data were collected using a data logger with an accuracy of approximately  $0.01^\circ\text{C}$  for temperature, 0.01 PSI for pressure, and 0.01 LPM for flow rate measurements.

Experimental methods establish the relationship between a parameter input, such as a flow rate, temperature, pressure, and fully developed conditions are controlled conditions. It is critical to manage experimental settings and the event itself precisely. Including a control group in experimental research is critical to ensure effective variable control. Figure 2 provided schematic test section in this study.

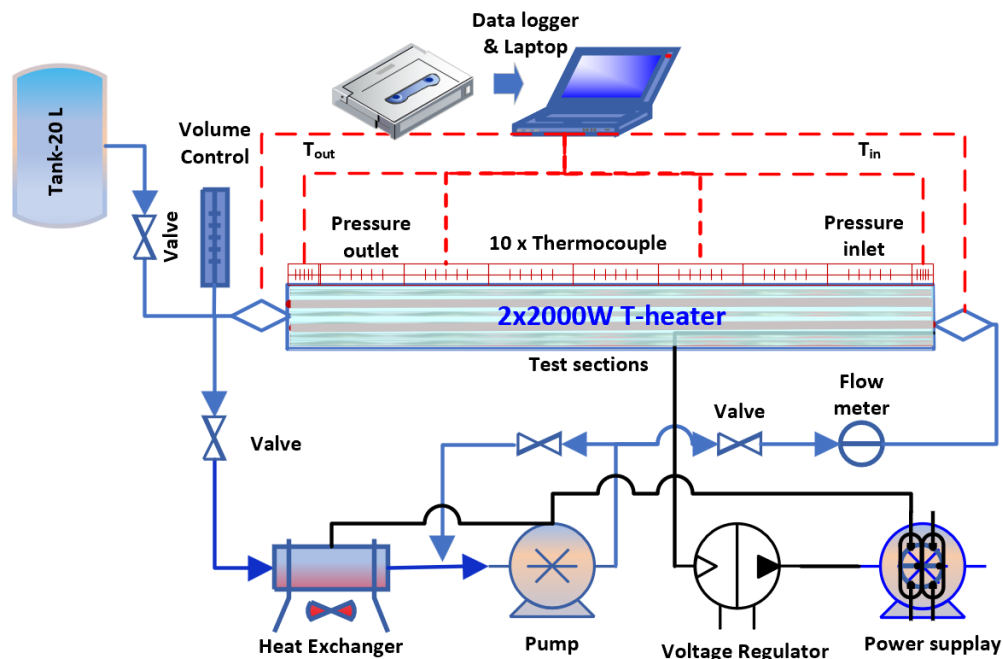


Figure 2. Experimental set up

## 2.3. Heat Transfer Coefficient (HTC), $h$

The HTC is a measurement of how well a material or surface can transfer heat from one location to another. It is commonly denoted as " $h$ " and is measured in  $\text{W}/\text{m}^2\text{K}$ . The HTC value depends on various factors, including the material's selected, the shape of the objects involved, the way fluids flow, and the temperature difference between them. This coefficient is especially valuable when calculating heat transfer in processes like convection or phase changes between liquids and solids. Equation 1 is typically used to determine its value [25].

$$h = \frac{Q}{T_s - T_m} \quad (1)$$

In this context, the temperature denoted as  $T_s$  represents the means temperature (K) of the surface being tested for suction. Its value is determined using Equation 2, as referenced in [25].

$$T_s = \frac{(\sum_{i=1}^8 T)}{10} \quad (2)$$

In this context,  $T_m$  stands for the bulk temperature (K) of the fluid, and its value is determined using Equation 3 [30].

$$T_m = \frac{T_{in} - T_{out}}{2} \quad (3)$$

The heat transfer rate ( $W$ ) in this study is determined through the use of Equation (4), as specified in [21].

$$Q = \frac{Q_1 + Q_2}{2} \quad (4)$$

In this context,  $Q_1$  represents for heat transfer rate ( $W$ ) originating from the power source used, and it is determined using Equation (5). On the other hand,  $Q_2$  is the heat transfer rate associated with the fluid's performance and is determined employing Equation (6), as indicated in reference [31].

$$Q_1 = VI \quad (5)$$

$$Q_2 = \dot{m}C_p(T_o - T_i) \quad (6)$$

where  $V$  for voltage (volts),  $I$  for current (Amperes),  $m'$  for mass flow rate (kg/s), and  $C_p$  for specific heat capacity (J/kg-K). Heat flux measures how quickly heat moves across a surface. It's expressed in watts per square meter ( $W/m^2$ ), which tells us how much heat flows through each square meter of that surface. To find heat flux using Equation 7, researchers usually measure these variables, and the specific method might differ based on the situation or the study's requirements. The equation and what exactly needs to be measured can be found in the specific reference or study being used [32].

$$q'' = \frac{Q}{\pi DL} \quad (7)$$

Where  $D$ , represented for inner diameter (m) of the pipe and  $L$ , which stands for the length of the pipe (m).

#### 2.4. Determination of Reynold Number ( $Re$ ) and Nusselt number ( $Nu$ )

The Reynolds number is a dimensionless parameter that encapsulates the relationship between two critical forces within a particular flow situation. It is calculated using Equation 8. Reynolds numbers serve as a valuable tool for categorizing various types of flow, including laminar, turbulent, and transitional flow. By evaluating the Reynolds number, engineers and scientists can determine the dominant flow regime in a given situation, which is crucial for understanding fluid behavior and optimizing designs in different applications [33].

$$Re = \frac{\rho v D}{\mu} \quad (8)$$

Where  $Re$  represents the dimensionless Reynolds number,  $v$  represents fluid velocity (m/s),  $\mu$  represents the absolute viscosity of the fluid (mPs), and  $\rho$  denotes fluid density ( $kg/m^3$ ) [34].

The Nusselt number ( $Nu$ ) is a parameter that characterizes convection heat transfer at a surface by quantifying the non-dimensional temperature gradient. In this experiment, the Nusselt number was determined using Equation 9. This parameter helps us understand how efficiently heat is being transferred at the surface, which is crucial in various heat transfer and fluid dynamics studies [35].

$$Nu = \frac{hD}{k} \quad (9)$$

Equation 10 was used to calculate the Nusselt number ( $Nu$ ). Moreover, the Nusselt numbers gained in this study were compared employing Bottler's Disstut formula (Equation 10) and Notter & Rouse's Equation 11. These evaluations and estimations aid in evaluating the system's efficiency and heat transfer coefficient under consideration, revealing valuable information about heat transfer performance [36, 37].



$$Nu = 0.023Re^{0.8}Pr^{0.4} \quad (10)$$

$$Nu = 5 + 0.015Re^{0.856}Pr^{0.347} \quad (11)$$

## 2.5. Pressure Drops and Friction Factor

Pressure drop is the reduction in energy that happens when a fluid encounters resistance while flowing through a pipe or channel. This resistance can result from factors like friction between the fluid and the pipe walls, alterations in flow velocity, or shifts in pipe geometry. Pressure drop is typically quantified in pressure units (Pascal). On the other hand, the friction factor gauges the impact of friction between the fluid and the pipe wall on fluid flow. It's commonly denoted as " $f$ " and plays a role in pressure drop calculations. The value of the friction factor fluctuates based on the regimes type (and the pipe's geometry).

The pressure drop is determined by subtracting the pressure differences at the system's inlet and outlet. The pressure drop ( $P$ ) is normally determined by employing Equation 12 [29, 38].

$$\Delta P = P_{in} - P_{out} \quad (12)$$

The Darcy friction factor is a dimensionless factor for assessing frictional losses in pipes. Equation 13 can be used to calculate the experimental friction factor. This parameter is critical for comprehending and quantifying fluid flow resistance, which is important for various engineering and fluid dynamics applications, particularly when determining pressure drops and losses in pipes [39].

$$f = \frac{\Delta P}{\left(\frac{L}{D}\right)\left(\rho_f \frac{v^2}{2}\right)} \quad (13)$$

Equations 14 and 15 show how to calculate the friction factor using the Petukhov and Blasius equations [40]. These alternative formulas provide ways of calculating the friction factor in specific flow conditions, providing useful tools for analyzing and predicting the behaviour of fluids in different situations [41, 42].

$$f = (0.79 \ln Re - 1.64)^{-2} \quad (14)$$

$$f = \frac{0.3164}{Re^{0.25}} \quad (15)$$

## 3. RESULT AND DISCUSSIONS

### 3.1. Analysis of Heat Transfer Coefficient (HTC), $h$

The  $HTC$  ( $h$ ) was determined from experimental data using Equation (1), and the results were averaged and analyzed to assess the impact of EG/Water fluid flow rate. The analysis revealed that  $h$  increases as  $Re$  of the fluid rises. The lowest  $HTC$  occurs at  $Re$  values in the range of 2000, while the highest is observed at  $Re$  values exceeding 8000. A substantial increase in  $HTC$  occurs within the  $Re$  range of 2000 to 4500 and between 6500 and 8000. Beyond this range, the increase in  $h$  is less pronounced. Figure 3 visually depicts the influence of  $Re$  variation on the  $HTC$ .

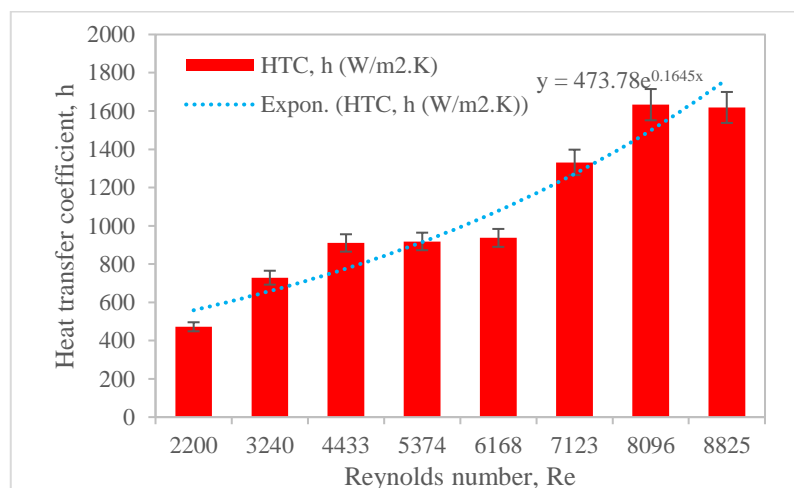


Figure 3. The effect of EG/Water fluid flow rate on the Nusselt number

The fluid flow rate's effect on the *HTC* was analyzed. The results demonstrate that the *HTC* rises as the fluid flow increases. The lowest *HTC* is observed at a fluid flow rate of 4 LPM, while the highest is at a *Re* exceeding 12 LPM. Figure 4 provides a clear visualization of the impact of variations in fluid flow rate on the *HTC*. The results of this study consistently support the basic theory, which indicates that the heat transfer rate is positively related (directly proportional) to the *HTC* (heat transfer coefficient), as documented in reference [25]. There is a strong understanding that the fluid flow rate influences the heat transfer rate [43, 44]. In the context of this research, it was found that the fluid mass flow rate also has a positive correlation (directly proportional) to the fluid flow rate used.

### 3.2. Analysis of the effect of Reynold number on Pressure drops

Pressure drop ( $\Delta P$ ) and friction factor ( $f$ ) calculations were performed using Equation 12. The calculated  $\Delta P$  results were then averaged and analyzed to comprehend the impact of *Re* variations in EG/Water fluid flow. Figure 5 illustrates the  $\Delta P$  increases as the *Re* in flowrate rises. The lowest  $\Delta P$  is observed when the *Re* around 2000, while the highest occurs when the *Re* surpasses 8500.

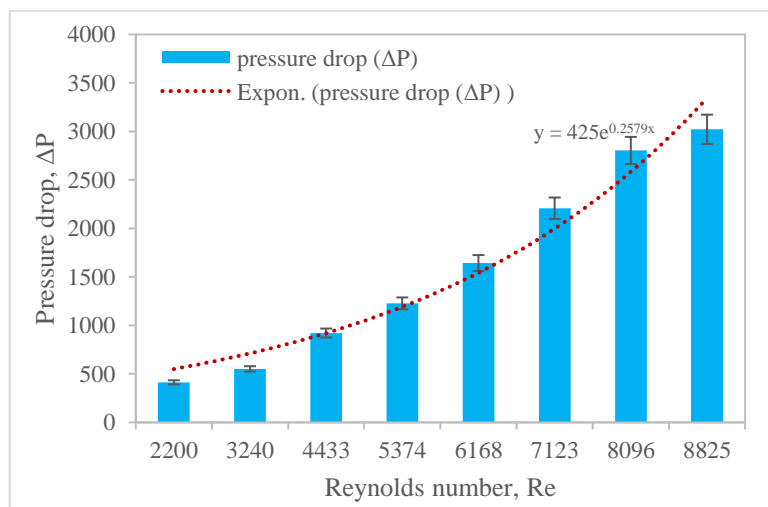


Figure 4. The effect of the EG/Water fluid flow rate on the heat transfer coefficient

The observation of a pressure drop that increases in tandem with the *Re* number is evident from Figure 5. The *Re* number is directly proportional to the fluid velocity and flow rate, which causes this phenomenon to occur. Consistent with the results documented by [36], which indicate that pressure drop increases with increasing flow rate and *Re* number, this instance also demonstrates an increase in pressure drop.

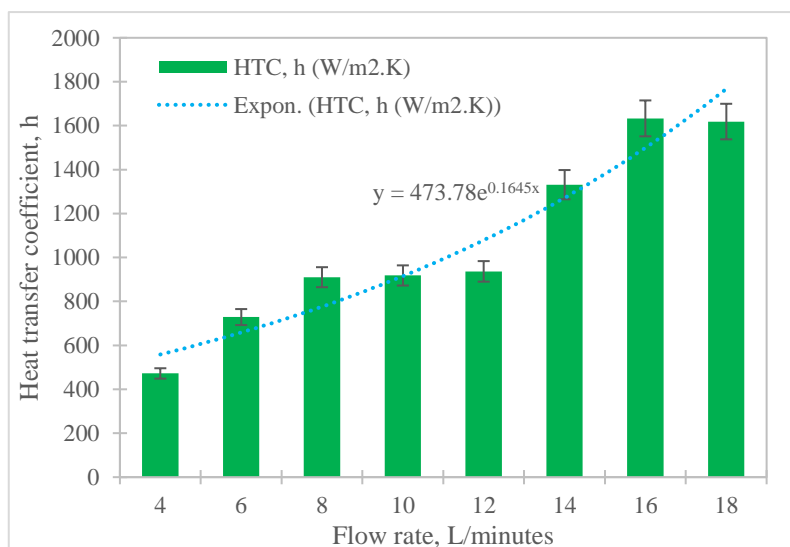


Figure 5. Effect of Reynolds number on Pressure drops.

### 3.3. Analysis of the effect of Reynold number on Friction factor

The friction factor ( $f$ ) was calculated using experimental data and compared to the Petukhov and the Blasius equation. Equation 13 was used to calculate the experimental friction factor, while Equations 14 and 15 were used to apply the Petukhov and Blasius formula direction [36]. Figure 6 depicts the effect of changes in the  $Re$  on the friction factor. The data show that as the  $Re$  in EG/Water fluid flow increases, so does the friction factor. The results of the friction factor calculations based on experimental data closely align with the Petukhov and Blasius formulas.

Figure 6 illustrates that the friction factor diminishes with escalating  $Re$  in the EG/Water fluid flow. The findings indicate that the highest friction factor is observed at a  $Re$  around 2000, while the lowest is recorded at a  $Re$  exceeding 8500. It suggests that, in the context of EG/Water fluid flow, the friction factor tends to decrease as the  $Re$  rises, reflecting the fluid flow characteristics within the system.

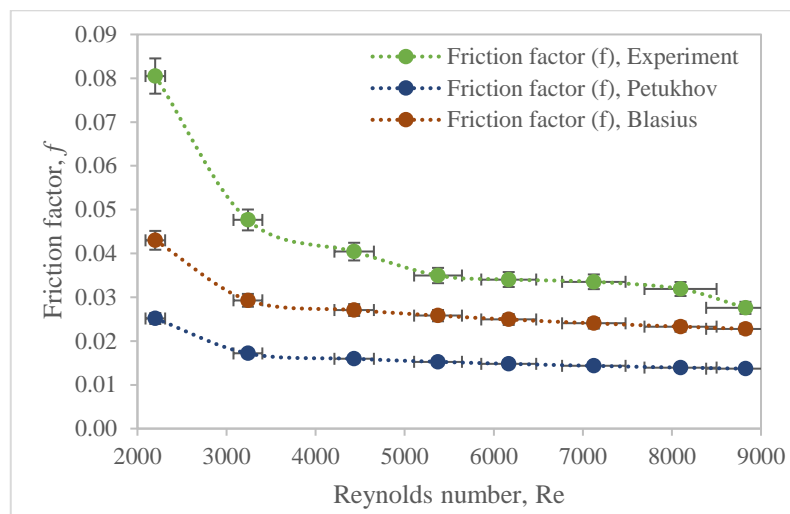


Figure 6. Effect of Reynolds number on Friction factor.

The outcomes of this research consistently affirm the fundamental theory, as corroborated by references [39] and [40], which establish a positive correlation (direct proportionality) between the friction factor value and both pressure drop and Reynolds number ( $Re$ ). It is widely acknowledged that the Reynolds number is influenced by velocity, as noted in reference [30], and fluid flow rate, as cited in reference [31]. In the specific context of this study, it was observed that fluid velocity and flow rate also exhibit a positive correlation (direct proportionality) with the Reynolds number. Consequently, the friction factor tends to decrease as the Reynolds number increases, signifying that an increase in fluid flow velocity and flow rate reduces the resulting pressure.

### 3.4. Analysis of Reynolds number ( $Re$ ) and Nusselt number ( $Nu$ )

The  $Re$  and  $Pr$  were determined using equations (8) and (9), and the resulted in averaged than analysed to examine the influence of fluid flow rate on these two dimensionless parameters. The research outcomes reveal that the  $Re$  and  $Pr$  numbers increase as the EG/Water fluid flow rates rise. The lowest Reynolds number was obser The  $Re$  and  $Pr$  at a flow rate of 4 LPM, while the highest occurred at 18 LPM. A similar pattern was observed for the Prandtl number, with the lowest value recorded at 4 LPM and the highest at 18 LPM. Figure 7 visually represents the data for the The  $Re$  and  $Pr$  numbers.

The  $Nu$  number evaluation is then compared with the Disstut Bottler (10) and Notter & Rouse (11) equations, with fluid flow rate considerations. Figure 8 depicts these comparative outcomes. The calculated results are then averaged and analyzed to determine the effect of flow rate on the Nusselt number. The results show that the  $Nu$  rises with flow rate, with the lowest value at 4 LPM and the highest at 18 LPM. The experimental data closely matches the  $Nu$  number calculation based on the Disstut Bottler equation but outperforms the Notter and Rouse formula.



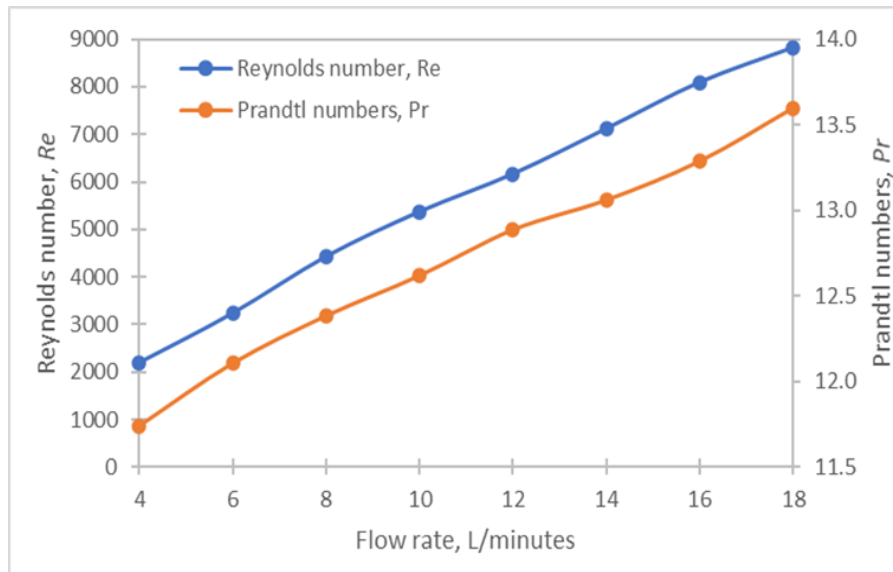


Figure 7. Effect of EG/Water fluid flow rate on Re and Pr.

The  $Nu$  number, as per equation (9) outlined in reference [35], demonstrates a positive correlation (direct proportionality) with the HTC, in line with the findings in reference [25]. Furthermore, the  $Nu$  number is closely linked to the Reynolds number ( $Re$ ), as reference [25, 36] indicates. It is well-established that the  $Nu$  number value is influenced by the fluid flow rate, as acknowledged in reference [31]. In this research, we have determined that the  $Nu$  number value of the fluid also exhibits a positive correlation (direct proportionality) with the fluid's flow rate. Therefore, an increase in the fluid flow rate leads to a corresponding increase in the  $Nu$  number, indicating a heightened heat transfer rate through the fluid.

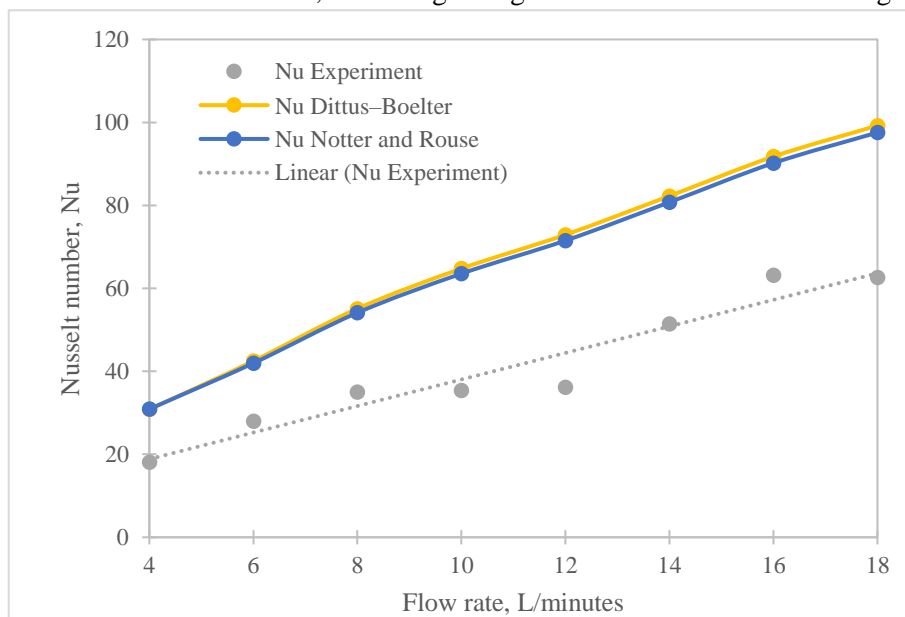


Figure 8. Effect of EG/Water fluid flow rate on the Nusselt number

#### 4. CONCLUSIONS

The research effectively examined heat transfer coefficients and pressure drop in copper pipe flow systems employing a 40:60 EG/water fluid mixture at a temperature of 60°C. Significant effects of fluid flow rate variations on HTC and pressure drop ( $\Delta P$ ) were observed. A positive correlation was observed between flow rate and HTC in the EG/Water fluid; as flow rate increased, HTC also increased. This correlation was observed to be associated with the simultaneous increase in the Reynolds number ( $Re$ ), which increases in tandem with higher flow rates and thus increases the heat transfer coefficient. On the contrary, the value of

$\Delta P$  in the fluid contained within the copper pipe exhibited a direct correlation with the rate of fluid flow, suggesting that higher flow rates resulted in a greater increase. It is noteworthy that as the flow rate increased, the friction factor in the EG/Water fluid decreased. In addition, a direct correlation was observed between the fluid flow rate and the Reynolds number of the fluid within the copper pipe.

## AUTHOR'S DECLARATION

### Authors' contributions and responsibilities

The authors played significant roles in conceiving and designing the study. The authors also took on the responsibility for data analysis, interpretation, and the discussion of results. All authors reviewed and gave their approval for the final manuscript.

### Acknowledgment

The author sincerely thanks the dedicated team at Laboratory of Energy Conversion Laboratory, Universitas Buana Perjuangan Karawang, for their invaluable assistance in data collection throughout the experimental process. Their support is immensely appreciated.

### Availability of data and materials

All data pertaining to this research are available from the authors upon request.

### Competing interests

The authors affirm that they have no competing interests to declare.

## REFERENCES

- [1] M. S. Liu, M. C. C. Lin, I. T. Huang, and C. C. Wang, "Enhancement of thermal conductivity with CuO for nanofluids," *Chemical Engineering and Technology*, vol. 29, no. 1, pp. 72-77, 2006.
- [2] M. A. Khatkhat, M. A., and S. Kamran Afalaq, "Application of nanofluids in heat exchangers: A review," *Journal of Advanced Research in Materials Science*, vol. 66, no. 1, pp. 5625-5638, 2020.
- [3] A. I. Ramadhan, W. H. Azmi, R. Mamat, and K. A. Hamid, "Experimental and numerical study of heat transfer and friction factor of plain tube with hybrid nanofluids," *Case Studies in Thermal Engineering*, vol. 22, no. April, pp. 100782-100782, 2020.
- [4] S. Sukarman and Y. S. Gaos, "Optimasi Desain Alat Penukar Kalor Gas Buang untuk Pemanas Air Degreaser," *Jurnal Ilmiah TEKNOBIZ*, vol. 8, no. 3, pp. 94-100, 2018.
- [5] M. Mehrpooya, M. Dehqani, S. A. Mousavi, and S. M. A. Moosavian, "Heat transfer and economic analyses of using various nanofluids in shell and tube heat exchangers for the cogeneration and solar-driven organic Rankine cycle systems," *International Journal of Low-Carbon Technologies*, vol. 17, no. November, pp. 11-22, 2022.
- [6] E. Borri *et al.*, "Phase Change Slurries for Cooling and Storage: An Overview of Research Trends and Gaps," *Energies*, vol. 15, no. 19, 2022.
- [7] R. LeSar and R. LeSar, "Materials selection and design," *Introduction to Computational Materials Science*, pp. 269-278, 2013.
- [8] H. Ibrahim, N. Sazali, A. S. M. Shah, M. S. A. Karim, F. Aziz, and W. N. W. Salleh, "A review on factors affecting heat transfer efficiency of nanofluids for application in plate heat exchanger," *Journal of Advanced Research in Fluid Mechanics and Thermal Sciences*, vol. 60, no. 1, pp. 144-154, 2019.
- [9] A. Ghozatloo, M. Shariaty-Niasar, and A. M. Rashidi, "Investigation of Heat Transfer Coefficient of Ethylene Glycol/ Graphenenanofluid in Turbulent Flow Regime," *Int. J. Nanosci. Nanotechnol.*, vol. 10, no. 4, pp. 237-244, 2014.
- [10] M. Bayareh, A. H. Pordanjani, A. A. Nadooshan, and K. S. Dehkordi, "Numerical study of the effects of stator boundary conditions and blade geometry on the efficiency of a scraped surface heat

- exchanger," *Applied Thermal Engineering*, vol. 113, pp. 1426-1436, 2017.
- [11] B. C. Pak and Y. I. Cho, "Hydrodynamic and Heat Transfer Study of Dispersed Fluids With Submicron Metallic Oxide," *Experimental Heat Transfer : A Journal of, Thermal Energy Transport, Storage, and Conversion*, vol. 11, no. 2, pp. 151-170, 2007.
- [12] L. Godson, K. Deepak, C. Enoch, B. R. Jefferson Raja, and B. Raja, "Heat transfer characteristics of silver/water nanofluids in a shell and tube heat exchanger," *Archives of Civil and Mechanical Engineering*, vol. 14, no. 3, pp. 489-496, 2014.
- [13] W. H. Azmi, K. V. Sharma, P. K. Sarma, R. Mamat, S. Anuar, and V. Dharma Rao, "Experimental determination of turbulent forced convection heat transfer and friction factor with SiO<sub>2</sub> nanofluid," *Experimental Thermal and Fluid Science*, vol. 51, pp. 103-111, 2013.
- [14] W. Zheng, H. Zhang, S. You, and T. Ye, "Numerical and experimental investigation of a helical coil heat exchanger for seawater-source heat pump in cold region," *International Journal of Heat and Mass Transfer*, vol. 96, pp. 1-10, 2016.
- [15] Z. Said, S. M. A. Rahman, M. El Haj Assad, and A. H. Alami, "Heat transfer enhancement and life cycle analysis of a Shell-and-Tube Heat Exchanger using stable CuO/water nanofluid," *Sustainable Energy Technologies and Assessments*, vol. 31, no. December 2018, pp. 306-317, 2019.
- [16] M. Setiyo, S. Soeparman, N. Hamidi, and S. Wahyudi, "Caractéristiques de l'effet refroidissant d'un système frigorifique à demi-cycle sur un système au GPL," *International Journal of Refrigeration*, vol. 82, pp. 227-237, 2017.
- [17] M. Hojjat, "Nanofluids as coolant in a shell and tube heat exchanger: ANN modeling and multi-objective optimization," *Applied Mathematics and Computation*, vol. 365, pp. 124710-124710, 2020.
- [18] A. R. Akeedy, H. Alias, and S. D. Salman, "Heat transfer enhancement using passive technique: Review," *Jurnal Teknologi*, vol. 83, no. 2, pp. 151-162, 2021.
- [19] I. M. Shahrul, I. M. Mahbubul, R. Saidur, S. S. Khaleduzzaman, M. F. M. Sabri, and M. M. Rahman, "Effectiveness study of a shell and tube heat exchanger operated with nanofluids at different mass flow rates," *Numerical Heat Transfer; Part A: Applications*, vol. 65, no. 7, pp. 699-713, 2014.
- [20] S. P. Louis, S. Ushak, Y. Milian, M. Nemés, and A. Nemés, "Application of Nanofluids in Improving the Performance of Double-Pipe Heat Exchangers—A Critical Review," *Materials*, vol. 15, no. 19, 2022.
- [21] N. Tamilselvan, M. Thirumarimurugan, and E. Sudalai Manikandan, "Study on various control strategies of plate type heat exchanger for non-Newtonian fluids," *Journal of Ambient Intelligence and Humanized Computing*, vol. 12, no. 7, pp. 7253-7261, 2021.
- [22] R. Andrzejczyk and T. Muszyński, "Performance analyses of helical coil heat exchangers. the effect of external coil surface modification on heat exchanger effectiveness," *Archives of Thermodynamics*, vol. 37, no. 4, pp. 137-159, 2016.
- [23] M. H. Rostami, G. Najafi, B. Ghobadin, and A. Motevali, "Thermal performance investigation of SWCNT and graphene quantum dots nanofluids in a shell and tube heat exchanger by using fin blade tubes," *Heat Transfer*, vol. 49, no. 8, pp. 4783-4800, 2020.
- [24] E. M. Go, E. Shin, J. H. Cha, and S. K. Kwak, "Estimation of heat transfer coefficient of water and ethylene glycol mixture in nanopipe via non-equilibrium coarse-grained molecular dynamics," *Journal of Industrial and Engineering Chemistry*, vol. 77, pp. 128-134, 2019.
- [25] T. U. H. S. G. Manik, G. Sudrajat, and T. B. Sitorus, "The experimental study of the coolant flow rate of an ethylene glycol-mixed water to the heat transfer rate on the radiator," vol. 505, pp. 0-8.
- [26] S. M. Abolarin, M. Everts, and J. P. Meyer, "Heat transfer and pressure drop characteristics of alternating clockwise and counter clockwise twisted tape inserts in the transitional flow regime," *International Journal of Heat and Mass Transfer*, vol. 133, pp. 203-217, 2019.
- [27] N. Azari, I. Chhaya, Y. Ghamat, D. Kanthariya, M. Patel, and F. Bodiwala, "Experimental

- Investigation of Heat Transfer in Compact Heat Exchanger using Water-Ethylene Glycol," vol. 8, no. 04, pp. 666-669, 2019.
- [28] T. Thiyana, J. Ahmad, A. R. Muhammad, S. Sukarman, K. Khoirudin, and R. I. Azizah, "Heat Transfer Coefficient in a Copper Pipe Flow System Using a 40/60 Volume Ratio Ethylene Glycol/Water (EG/H<sub>2</sub>O) Blended Fluid," *Jurnal Teknik MesinMechanical Xplore (JTMMX)*, vol. 1, no. 2, pp. 37-46, 2023.
- [29] W. Ajeeb, R. R. S. Thieleke da Silva, and S. M. S. Murshed, "Experimental investigation of heat transfer performance of Al<sub>2</sub>O<sub>3</sub> nanofluids in a compact plate heat exchanger," *Applied Thermal Engineering*, vol. 218, pp. 119321-119321, 2023.
- [30] S. N. M. Zainon and W. H. Azmi, "Heat Transfer Performance of Green Bioglycol-Based TiO<sub>2</sub>-SiO<sub>2</sub> Nanofluids," *Journal of Heat Transfer*, vol. 143, no. 11, pp. 1-10, 2021.
- [31] W. H. Azmi, K. V. Sharma, P. K. Sarma, R. Mamat, and G. Najafi, "Heat transfer and friction factor of water based TiO<sub>2</sub> and SiO<sub>2</sub> nanofluids under turbulent flow in a tube," *International Communications in Heat and Mass Transfer*, vol. 59, pp. 30-38, 2014.
- [32] L. Karikalán, S. Baskar, N. Poyyamozi, and K. Negash, "Experimental Analysis of Heat Transfer by Using Nanofluid and Impact of Thermophysical Properties," *Journal of Nanomaterials*, vol. 2022, 2022.
- [33] A. Aghaei, "Thermal-hydraulic analysis of Syltherm 800 thermal oil /  $\gamma$ -AlOOH nanofluid in a baffled shell and tube heat exchanger equipped with corrugated helical tube with two-phase approach," *Engineering Analysis with Boundary Elements*, vol. 146, no. October 2022, pp. 668-694, 2023.
- [34] N. Arora and M. Gupta, "An experimental study on heat transfer and pressure drop analysis of Al<sub>2</sub>O<sub>3</sub>/water nanofluids in a circular tube," *Materials Today: Proceedings*, no. xxxx, pp. 2-7, 2022.
- [35] A. Alimoradi and F. Veysi, "Prediction of heat transfer coefficients of shell and coiled tube heat exchangers using numerical method and experimental validation," *International Journal of Thermal Sciences*, vol. 107, pp. 196-208, 2016.
- [36] M. R. Salem, R. K. Ali, R. Y. Sakr, and K. M. Elshazly, "Effect of  $\gamma$ -Al<sub>2</sub>O<sub>3</sub>/water nanofluid on heat transfer and pressure drop characteristics of shell and coil heat exchanger with different coil curvatures," *Journal of Thermal Science and Engineering Applications*, vol. 7, no. 4, pp. 1-9, 2015.
- [37] P. Zainith et al., "Heat transfer analysis of a shell and tube heat exchanger operated with graphene nanofluids," *Applied Thermal Engineering*, vol. 18, no. September 2020, pp. 238-247, 2020.
- [38] M. Bahiraei, M. Hangi, and M. Saeedan, "A novel application for energy efficiency improvement using nanofluid in shell and tube heat exchanger equipped with helical baffles," *Energy*, vol. 93, pp. 2229-2240, 2015.
- [39] R. Barzegarian, A. Aloueyan, and T. Yousefi, "Thermal performance augmentation using water based Al<sub>2</sub>O<sub>3</sub>-gamma nanofluid in a horizontal shell and tube heat exchanger under forced circulation," *International Communications in Heat and Mass Transfer*, vol. 86, pp. 52-59, 2017.
- [40] S. N. M. Zainon, W. H. Azmi, and A. H. Hamisa, "Thermo-physical Properties of TiO<sub>2</sub>-SiO<sub>2</sub> Hybrid Nanofluids Dispersion with Water/Bio-glycol Mixture," *Journal of Physics: Conference Series*, vol. 2000, no. 1, 2021.
- [41] R. Gugulothu and N. Sanke, "Use of segmental baffle in shell and tube heat exchanger for nano emulsions," *Heat Transfer*, vol. 51, no. 3, pp. 2645-2666, 2022.
- [42] B. Kristiawan, K. Enoki, W. E. Juwana, R. A. Rachmanto, A. T. Wijayanta, and T. Miyazaki, "Simulation-based assessment of the thermal-hydraulic performance of titania-based nanofluids in a circular-mini-channel tube," *International Journal of Ambient Energy*, vol. 43, no. 1, pp. 8022-8035, 2022.
- [43] S. V. Sridhar, R. Karuppasamy, and G. D. Sivakumar, "Experimental Investigation of Heat Transfer Enhancement of Shell and Tube Heat Exchanger Using SnO<sub>2</sub>-Water and Ag-Water Nanofluids,"

- Journal of Thermal Science and Engineering Applications*, vol. 12, no. 4, pp. 1-6, 2020.
- [44] I. M. Shahrul, I. M. Mahbubul, R. Saidur, and M. F. M. Sabri, "Experimental investigation on Al<sub>2</sub>O<sub>3</sub>-W, SiO<sub>2</sub>-W and ZnO-W nanofluids and their application in a shell and tube heat exchanger," *International Journal of Heat and Mass Transfer*, vol. 97, pp. 547-558, 2016.